PERGAMON

Planetary and Space Science 48 (2000) 41–49

Planetary and Space Science

Perpendicular electron heating by absorption of auroral kilometric radiation

D.D. Morgan[a,*], J.D. Menietti[a], R.M. Winglee[b], H.K. Wong[c]

[a]*Department of Physics and Astronomy, University of Iowa, Iowa City, IO 52242, USA*
[b]*Geophysics Program AK50, University of Washington, Seattle, WA 98195, USA*
[c]*Aurora Science Inc, San Antonio, TX 78228, USA*

Received 30 November 1998; received in revised form 12 April 1999; accepted 27 May 1999

Abstract

We investigate the possibility of perpendicular heating of electrons and the generation of quasiperpendicular (type 2) electron conics by particle diffusion in velocity space due to wave–particle interaction with intense auroral kilometric radiation. By introducing a ring distribution and a warm plasma dispersion relation, we conduct a basic simulation of conditions near an auroral kilometric radiation (AKR) source. We then solve the diffusion equation using a finite difference algorithm. The results show significant perpendicular electron heating as might exist adjacent to the AKR source region and indicate that the main characteristics of a quasiperpendicular (type 2) electron conic distribution can be reproduced under these conditions.

1. Introduction

Electron conics appear as enhancements in the particle flux just outside of the loss cone. Often they are the most energetic particle flux and appear as parallel stripes on an energy-time spectrogram. A number of authors have discussed the generation mechanisms for electron conical distributions since their discovery in the DE-1 data set by Menietti and Burch (1985), who observed the electron conics associated with trapped particles and parallel electric fields and suggested a wave–particle interaction and perpendicular heating as a source mechanism, analogous to ion conic formation.

There is a growing consensus that while some electron conics may be generated by upper hybrid waves, the majority of the examples are associated with parallel electric field oscillations at low-frequency (cf Andre, 1993; Andre and Eliasson, 1992; Eliasson et al., 1996; Menietti and Weimer, 1998; Menietti et al., 1992; Thompson and Lysak, 1996).

If we refer to the electron conics described above as "type 1", there is another class of "electron conic" that appears as an enhancement in the electron phase space distribution function centered at a pitch angle of 90°, which we will call "type 2". An example of this type of distribution was reported near the source region of auroral kilometric radiation (cf Fig. 3b, Menietti et al., 1993). A brief review of electron conics including the "90°" conics was given by Menietti (1992). Menietti et al. (1994) have suggested that it may be possible for some type 2 electron conics to evolve into type 1 as the electrons move up the magnetic field line and "fold" to smaller pitch angles due to conservation of the first adiabatic invariant. The mechanism for the production of type 2 electron conics has been suggested as electron heating by auroral kilometric radiation (Menietti et al., 1994), particularly in light of observations of strong temperature anisotropies ($T_\perp/T_\parallel > 10$) associated with electrons distributions near AKR source centers (cf Menietti et al., 1993). Recent observations of the FAST satellite

* Corresponding author.

0032-0633/00/$20.00
PII: S0032-0633(99)00079-3

within the AKR source region (Delory et al., 1998) have clearly shown the presence of anisotropic distributions ($T_\perp \gg T_\parallel$), and the authors have suggested that AKR could be the source of the perpendicular electron heating.

Auroral kilometric radiation is commonly observed at spectral densities of up to 10^{-9} $(V/m)^2/Hz$ (Gurnett, 1974) and frequencies up to several hundred kilohertz and down to the R-X cutoff (Bahnsen et al., 1989; Benson and Calvert, 1979; Gurnett et al., 1983). Benson and Calvert (1979) find that the wave normal angle is probably close to 90°. In source regions, AKR is observed to exist at frequencies below the local electron cyclotron frequency (cf Bahnsen et al., 1989; Menietti et al., 1993; Delory et al., 1998). This occurrence is due to the presence of a relativistic plasma distribution, which can drive the R-X cutoff below the electron cyclotron frequency (cf Winglee, 1985). Ungstrup et al. (1990) have shown that the loss cone in the AKR source region is filled in and have hypothesized that this effect is due to fast diffusion brought about by a wave–particle interaction. Recent observations of the FAST satellite (cf Delory et al., 1998) have also indicated the existence of trapped electrons near and perhaps within the AKR source region. The question arises, are these trapped electrons a source of AKR growth (cf Louarn et al., 1990) or a result of wave–particle heating? Electron heating for the case of radio wave absorption in solar coronal loops has been discussed in the past (cf Vlahos et al., 1982), but similar work for the case of terrestrial AKR is not so abundant. In the present paper, we do not calculate AKR wave growth, but rather examine the hypothesis that fast electron diffusion due to interaction of the electron distribution with AKR can cause the quasi-perpendicular electron conic distributions observed by Dynamics Explorer, as proposed by Ungstrup et al. (1990) and Menietti et al. (1994).

Wu et al. (1981) approximate the diffusion coefficient for conditions applicable to fundamental R-X mode AKR. Using this approximation, we estimate the value of the diffusion coefficient and compute representative diffusion times for various distributions. To simulate the action of diffusion on a particle distribution, a finite difference algorithm is then used to solve the diffusion equation given by Wu et al. (1981). We shall show that perpendicular electron heating can be reproduced under conditions approximating those in the AKR source region.

We emphasize that this work is not intended to be a rigorous, self-consistent (i.e., quasilinear) analysis, but only a feasibility study, with the purpose of presenting a reasonable explanation for wave observations. We leave the task of a more comprehensive approach to future investigators.

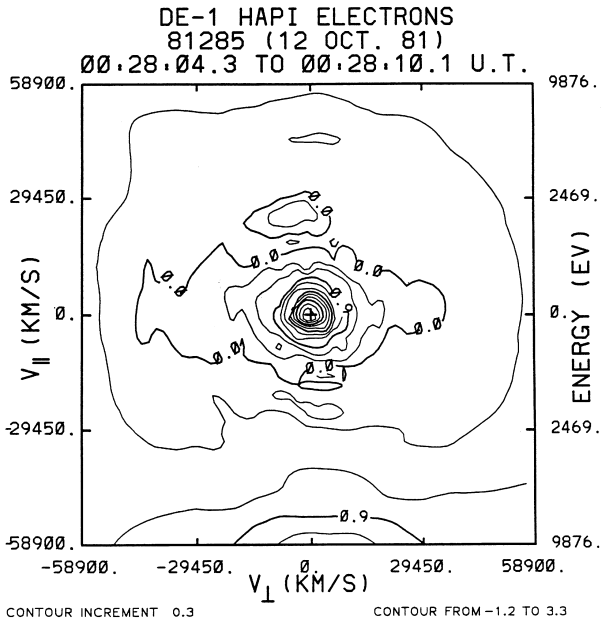

Fig. 1. Contour plot of the electron distribution function on day 285 at 00:28:04 UT, poleward of an AKR source region. This contour shows perpendicular heating of the low temperature distribution out to about 4.5 keV. (From Menietti et al., 1993.)

2. Observations

Plate 2 of Menietti et al. (1993) shows a time-frequency spectrogram of an AKR event observed near the source region at an unusually high altitude in the nightside auroral region by DE 1 on 12 October 1981. Two spacecraft positions where intense AKR emission extends below the local electron cyclotron frequency are indicated on the spectrogram, one at 00:28:30 universal time (UT) and the other at 00:29:30 UT. Menietti et al. (1993) (cf Bahnsen et al., 1987, 1989) conclude that the spacecraft intersects source field lines at these times. Adjacent to the source region, the authors observed particle distributions with $T_\perp/T_\parallel > 1$, possibly due to wave–particle interactions leading to perpendicular diffusion. This region extends about one-half degree in invariant latitude poleward of the observed source regions.

Fig. 1 of the present paper shows a contour plot of a perpendicularly heating electron distribution occurring adjacent to and poleward of the source region observed in the aforementioned event at 00:28:30 UT. This figure shows a distinct enhancement of the electron distribution perpendicular to the magnetic field extending to about 4.5 keV. The electron distribution extends to about 0.6 keV in the parallel direction. There is also a clear filling in of the loss cone. We believe that the elongation of the distribution in the perpendicular direction and the filled-in loss cone are the result of a wave–particle interaction involving

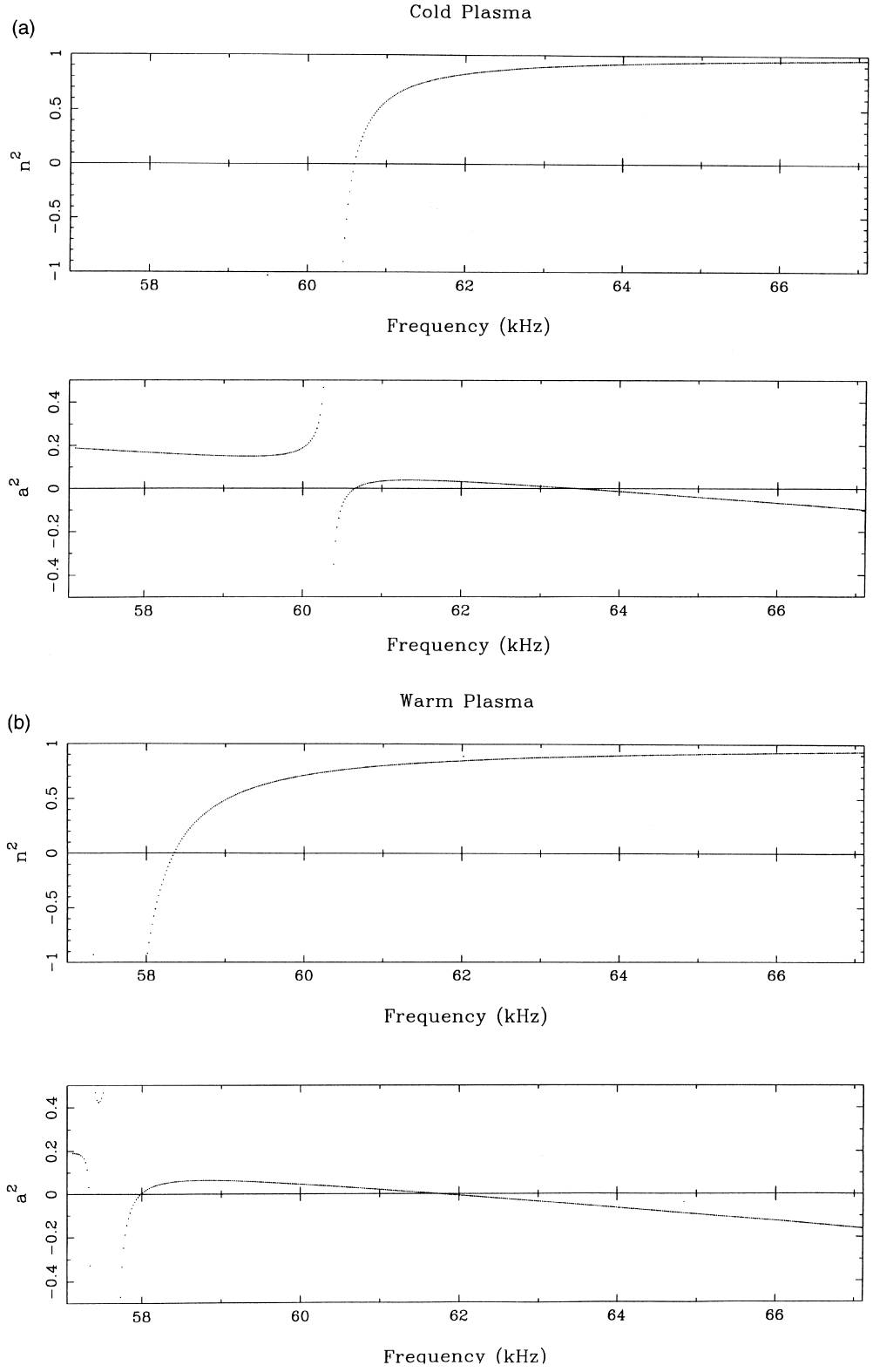

Fig. 2. (a) (Top) The square of the index of refraction and (bottom) the square of the semimajor axis of the resonant ellipse are plotted against frequency. Plasma parameters as explained in the text are $\psi = 90^\circ$, $f_{ce} = 60$ kHz, $f_{pc} = 6$ kHz, and $f_{pe} = 0$. kHz. The R-X cutoff can be seen to be about 60.6 kHz. The value of a^2 is greater than zero between about 60.7 and 63.4 kHz. Thus, resonant ellipses cannot be centered on the origin of velocity space. For this reason, resonant heating of electrons is impossible in this case. (b) (Top) The square of the index of refraction and (bottom) the square of the semimajor axis are plotted against frequency for a displaced ring delta function distribution given by Eq. (6). Plasma parameters as explained in the text are $f_c = 60$ kHz, $f_{pc} = 0$, $f_{pe} = 9$ kHz, $\beta_{||} = 0.3$, $\beta_\perp = 0.1$. The R-X cutoff is now seen to be 58.3 kHz. The frequency range in which a^2 is greater than zero is 58.0 to 61.8 kHz. Thus, resonant ellipses can be centered at the origin of velocity space.

intense AKR. This example is very similar to more recent examples obtained by the FAST instrument within the AKR source region (cf Fig. 2 of Delory et al., 1998). We shall attempt to reproduce these effects by modeling the radiation spectrum, the electron distribution, and the diffusion process.

3. The diffusion coefficient, index of refraction, and resonant ellipse

For the case of weak turbulence, the diffusion coefficient for R-X mode waves propagating nearly perpendicular to the magnetic field is given by Wu et al. (1981) as

$$D_{\perp\perp}(v_\perp, v_\parallel) = \frac{4\pi^2 e^2}{m^2}\int \mathrm{d}^3\mathbf{k}\, \mathscr{E}_k(t)\delta[\omega_\mathrm{r} - \Omega_\mathrm{c}/\gamma - k_\parallel v_\parallel] \quad (1)$$

where $\mathscr{E}_k(t)$ is electric wave energy per mode given here as a function of time, $\mathbf{k}$ is the wavevector, ω_r is the real part of the wave frequency, $\gamma = 1/\sqrt{(1 - v_\perp^2/c^2 - v_\parallel^2/c^2)}$, and Ω_c is the absolute value of the electron cyclotron frequency. For $|\mathbf{k}_\parallel v_\parallel|/\omega_\mathrm{r} \ll 1$, the evolution of the electron distribution function is given by the following equation from Wu et al. (1981)

$$\frac{\partial f_\mathrm{e}}{\partial t} = \frac{1}{v_\perp}\frac{\partial}{\partial v_\perp}\left[D(v_\perp, v_\parallel)v_\perp\frac{\partial f_\mathrm{e}}{\partial v_\perp}\right] \quad (2)$$

In this study we are only interested in an order-of-magnitude estimate of the saturation wave energy, and we do not consider the effect of the wave–particle interaction on the wave intensity (i.e., we do not do a full quasi-linear analysis), so that the wave energy per mode is considered to be constant. As discussed in Wu et al. (1981) this approximation is not bad because the X-mode growth rate is approximately constant over a large fraction of the saturation time.

Setting the argument of the delta function in Eq. (1) equal to zero for a given plasma frequency, cyclotron frequency, and wave normal angle, yields the resonant ellipse, which is the locus of points in velocity space that can interact with the wave at a given frequency. Particles not on a resonant ellipse do not interact with the wave. The parameters of the resonant ellipse are given by Melrose et al. (1982) in units of c as

$$C_1 = \frac{\omega \mathrm{k}_\parallel c}{\mathrm{k}_\parallel^2 c^2 + (\Omega_\mathrm{c})^2} \quad (3)$$

$$a = \left\{\frac{\mathrm{k}_\parallel^2 c^2 + (\Omega_\mathrm{c})^2 - \omega^2}{\mathrm{k}_\parallel^2 c^2 + (\Omega_\mathrm{c})^2}\right\}^{1/2} \quad (4)$$

and

$$b = \left\{\frac{(\Omega_\mathrm{c})^2}{\mathrm{k}_\parallel^2 c^2 + \Omega_\mathrm{c}^2}\right\}^{1/2} a \quad (5)$$

where C_1 is the displacement of the center of the ellipse along the $v_\parallel/c$-axis, a is the semimajor axis, b is the semiminor axis. We have set the harmonic number equal to 1.

Using ISIS 1 data, Benson and Calvert (1979) determined observationally that AKR has a low-frequency cutoff at the R-X cutoff frequency. However, as mentioned above, Viking, DE 1, and now FAST observations frequently show that the low-frequency cutoff of AKR can reach below the electron cyclotron frequency in the source region, indicating that the R-X cutoff frequency has been lowered due to the presence of relativistic electrons, as shown by Winglee (1985). This effect is crucial for the existence of perpendicular electron heating by AKR.

In order to simulate the effect of a relativistic electron distribution without a full distribution function calculation, we use a "displaced ring" distribution function consisting of a product of two delta functions:

$$f_\mathrm{e}(v_\perp, v_\parallel) = n_\mathrm{e}\frac{1}{2\pi v_\perp}\delta(v_\perp - v_{\perp 0})\delta(v_\parallel - v_{\parallel 0}) \quad (6)$$

This distribution function is analytically tractable for obtaining an approximation to the value of $D_{\perp\perp}$ [Eq. (1)]. Later in Section 4 when we numerically solve the diffusion equation (2), we will introduce a more realistic distribution function. Consistent with theory and past observations (cf Winglee 1985; Wong et al., 1982) we assume that the wave normal angle is near 90° in a low density plasma.

By using the formalism of Winglee (1985), Appendix A, for low density plasma, wave normal angle near 90°, and distribution function of Eq. (6) above, we find the following expression $n^2 = (S^2 - D^2)/S$, for the index refraction, where $S = 1 + Q_\mathrm{c} + Q_1 + Q_{-1}$ and $D = (\Omega_\mathrm{e}/\omega)Q_\mathrm{c} + Q_1 - Q_{-1}$, and where

$$Q_\mathrm{c} = -\frac{\omega_\mathrm{pc}^2}{\omega^2 - \Omega_\mathrm{e}^2} \quad (7)$$

and

$$Q_{\pm 1} = -\frac{1}{2}\frac{\omega_\mathrm{pc}^2}{\omega^2}\left[\omega^2 \mp \omega\Omega_\mathrm{c}\left(1 - \frac{1}{2}\frac{v_{\parallel 0}^2}{c^2}\right)\right]/\Delta_\pm \quad (8)$$

with definitions ω_pe is the energetic electron plasma

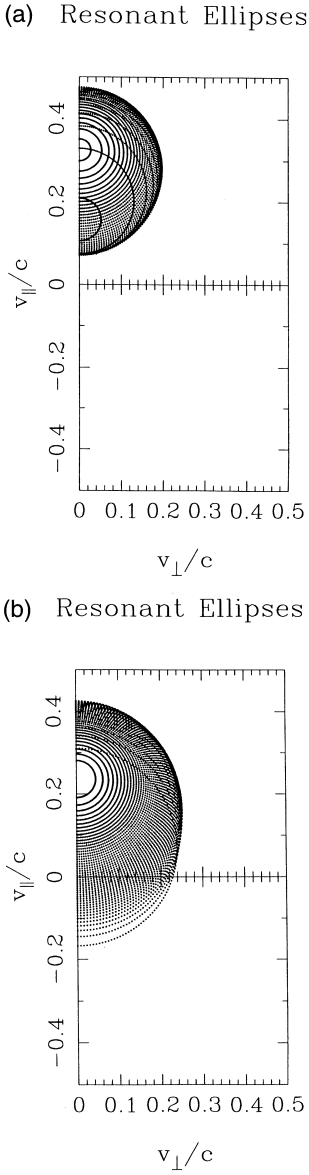

Fig. 3. (a) Resonant ellipses corresponding to the region of positive semimajor axis squared shown in Fig. 2(a). Note that the range of $v_\parallel/x$ is about 0.1 to 0.5c. Thus, the area around the origin of velocity space cannot interact with the wave and heating cannot occur. (b) Resonant ellipses corresponding to positive values of a^2 in Fig. 2(b). These resonant ellipses encompass the origin of velocity space and can, therefore, lead to interaction of AKR waves with cold particle distributions.

frequency, ω_{pc} is the cold electron plasma frequency, and $\Delta_\pm = \omega \mp \Omega_c/\gamma$.

We note that this treatment of the index of refraction applies for a wave normal angle close to 90°, but the index of refraction will not vary significantly either qualitatively or quantitatively for wave normal angles in the range $75° < \psi < 90°$ (cf Fig. 14, Wong et al., 1982). Therefore, in the following computations we will always compute the index of refraction using $\psi = 90°$ as an adequate approximation. Wave normal angles cited will refer to the angle used to compute $k_\perp$ and $k_\parallel$ in Eqs. (1) and (3)–(5).

In Fig. 2 we display the effect of varying the distribution function on the index of refraction (top panels) and the semimajor axis of the resonant ellipse (bottom panels). Fig. 2(a) shows these two quantities as a function of frequency for parameters wave normal angle $\psi = 70°$, cyclotron frequency $f_c = 60$ kHz, cold plasma frequency $f_{pc} = 6$ kHz, and energetic plasma frequency $f_{pe} = 0$ kHz. The top panel indicates that the R-X cutoff frequency is $f_{RX} = 60.6$ kHz. The bottom panel shows that the frequency range for which the square of the semimajor axis has positive values is 60.63 kHz $< f <$ 63.40 kHz. Resonant ellipses do not exist for frequencies outside of this range for the R-X mode, at the specified plasma frequency, cyclotron frequency, and wave normal angle.

In Fig. 2(b) we display the index of refraction and semimajor axis for parameters $\psi = 75°$, $f_c = 60$ kHz, $f_{pc} = 0$ kHz, and $f_{pe} = 9$ kHz. We note that recent FAST observations indicate that the cold plasma population can be quite low in the AKR source region (cf Strangeway et al., 1998). In Eq. (6) we set $v_{\perp 0}/c = 0.1$, and $v_{\parallel 0}/c = 0.3$. In the top panel of Fig. 2(b), the R-X cutoff frequency has been decreased to 58.3 kHz. The range in which the square of the semimajor axis is positive has been lowered to 58.0 kHz $< f <$ 61.8 kHz. The semimajor axis is now greater than zero at the R-X cutoff frequency ($f_{RX} = 59.4$ kHz) and reaches larger values than in Fig. 2.

The parallel velocity in the foregoing example is, therefore, large but not unreasonable for auroral plasma. In using our simplified approximation to the particle distribution, we found that $f_{RX} > f_c$ unless we assume a substantial parallel velocity of the electron distribution. This is not the case for a more realistic particle distribution, as shown in Fig. 1 of Winglee (1985). In that study, a Dory, Guest, and Harris (DGH) distribution (Dory et al., 1965) was used with reasonable auroral region parameters to give $f_{RX} < f_c$.

Fig. 3 shows several resonant ellipses corresponding to the parameters of Fig. 2. In Fig. 3(a), corresponding to Fig. 2(a), the size of the ellipses decreases to zero as the frequency approaches its limit at either end of the range for which $a^2 > 0$. Also, the resonant ellipses occur only in the $v_\parallel > 0$ half plane, as expected from Wu (1985). Because none of the resonant ellipses contain the region where $v_\parallel/c \approx 0$, the wave cannot interact with the low-energy particles in this region, and perpendicular heating cannot be produced. However, lowering the R-X cutoff frequency, as shown in Fig. 2 of this paper and in Fig. 1 of Winglee (1985), has the effect of changing the positions of the resonant ellipses. Fig. 3(b) shows this effect in detail. The resonant ellipse corresponding to $n = 0$ is now centered on the

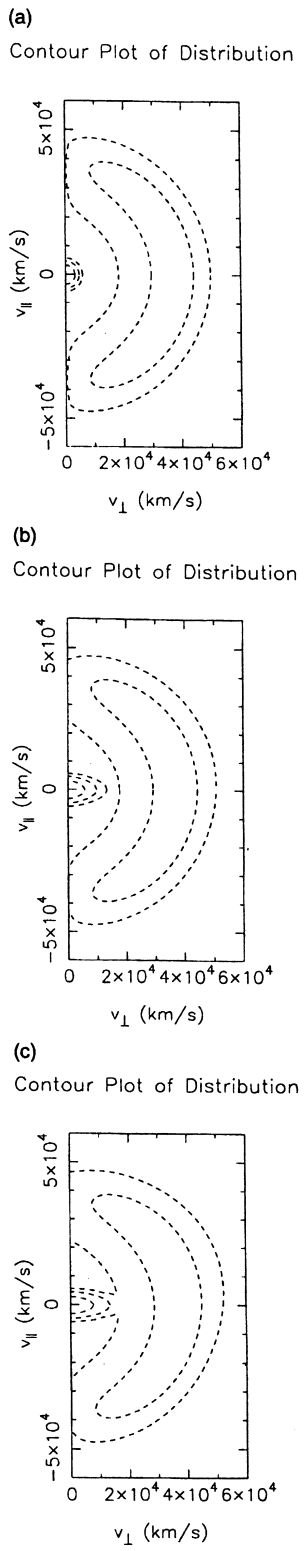

Fig. 4. (a) The initial distribution function used for the simulation run. This initial distribution consists of a Maxwellian distribution of thermal energy 2.5 eV added to a ring distribution of the form given in Eq. (11) with $v_0 = 0.125c$ and $\alpha_{loss} = 40°$. (b) The result of evolution of the initial distribution function shown in the previous figure after evolution for $1\tau_{diff}$, where $\tau_{diff} = 0.04$ s. The simulation reproduces the essential features of Fig. 1 elongation of the cold plasma distribution in the perpendicular direction, and filling in of the loss cone. (c) The result of evolution of the initial distribution shown in Fig. 4(a) for $3\tau_{diff}$, assuming that the spectral density can be much higher than measured by DE.

origin, in agreement with Eq. (3). The resonance ellipses for the interval 58.3 kHz $< f <$ 61.8 kHz are shown in Fig. 3(b) to encompass the origin and to reach about $0.23c$ along the perpendicular axis of velocity space, enough to include the region where electrons are heated in Fig. 1.

We have shown that a downward shift in f_{RX}, due, for example, to the presence of relativistic electrons, can lead to resonant ellipses that include the region around the origin of velocity space. Because the resonant ellipses tell us where wave-induced electron diffusion is possible, it is in such regions of velocity space that we can expect perpendicular diffusion of electrons, leading to heating and the formation of quasiperpendicular electron conics.

4. Diffusion model

We make two major assumptions in order to simplify calculation of the diffusion coefficient given by Eq. (1). First, as above, we assume that the AKR is emitted at a single wave normal angle near 90°. Second, we specify $f_c = 60$ kHz and $f_0 = 6$ kHz for all cases, similar to observed values from Menietti et al. (1993).

We approximate $\mathrm{d}|E|^2/\mathrm{d}\omega$ the power spectral density of AKR by

$$\frac{\mathrm{d}|E|^2}{\mathrm{d}\omega} = A\left\{\frac{f - f_{RX}}{\chi}\exp\left[-\left(\frac{f - f_{RX}}{\chi}\right)^2\right]\right\} \tag{9}$$

where $f > f_{RX}$ and A and χ are free parameters, A determining the maximum value and χ the bandwidth. For the simulation, we have chosen $\chi = 5$ kHz and $A = (2e)^{1/2} \times 10^{-9}$ $(\mathrm{V/m})^2/\mathrm{Hz}$, so as to give a typical peak spectral density of 10^{-9} $(\mathrm{V/m})^2/\mathrm{Hz}$. When this expression is inserted in Eq. (1), after expressing $\mathscr{E}_k(t)$ in terms of $\mathrm{d}|E|^2/\mathrm{d}\omega$, the electric energy density, we have

$$D_{\perp\perp} = \frac{4\pi^2 e^2}{m^2}\int \mathrm{d}\omega\epsilon_0 A\left(\frac{\omega - \omega_{RX}}{2\pi\chi}\right)^2 \mathrm{e}^{-[(\omega-\omega_{RX})/2\pi\chi]}\delta(\omega_r - \Omega_c/\gamma - k_\parallel v_\parallel) \tag{10}$$

We now show that the model assumed for the dispersion relation in the last section can be used to generate with $T_\perp \gg T_\parallel$ distributions for an electron

population in the presence of intense AKR. The simplified ring distribution, Eq. (6), was introduced to facilitate the calculation of $D_{\perp\perp}$. For the numerical simulation of plasma heating as described by Eq. (2), however, we introduce a more realistic plasma distribution. We assume the electron population is physically adjacent to the AKR source region, as observed, and can be described by two components. The first component is a cold Maxwellian of fixed energy, the value of which will be discussed in the next paragraph. The second component is a "ring distribution" with radius of v_0 and a loss cone α_{loss}, which we assume to have the form

$$f = \left[1.0 - \exp\left\{\frac{-1}{\alpha_{\text{loss}}}\sin^{-1}\left(\frac{v_\perp}{\sqrt{v_\perp^2 + v_\parallel^2}}\right)\right\}\right] \exp\left\{\frac{v_\perp^2 + v_\parallel^2 - v_0^2}{v_0^2}\right\} \tag{11}$$

where we have chosen $\alpha_{\text{loss}} = 40^\circ$ and $v_0 = 0.125c$. We stress that this distribution is not that of Eq. (6), which was introduced for analytical expediency in the calculation of $D_{\perp\perp}$. A contour plot of this initial distribution is shown in Fig. 4. We consider this distribution to be a cool component superimposed on the relativistic distribution bringing about the condition $f_{\text{RX}} < f_{\text{ce}}$. We then introduce the condition of saturation. As explained by Wu et al. (1981) the saturation time for AKR can be estimated by

$$t_{\text{sat}} = \frac{15}{10^{-3}\Omega_{\text{c}}}$$

With $\Omega_{\text{c}} = (2\pi)$ 60 kHz, we get $t_{\text{sat}} = 0.04$ s. The saturation time represents an upper limit on the time scale of any phenomena requiring the existence of AKR. Thus, the diffusion time for the formation of electron conics is expected to be 0.04 s or less. Diffusion time is given by

$$\tau_{\text{diff}} = \frac{v_{\text{th}}^2}{D_{\perp\perp}}$$

Since it is the cold plasma distribution that will primarily be subject to heating, we choose it to give the appropriate saturation time. It is found that a central Maxwellian of 2.5 eV gives $t_{\text{sat}} = 0.04$ s.

With the stated conditions, we have solved Eq. (2) with a finite difference algorithm for two different sets of parameters. The time increment is $10^{-3}\tau_{\text{diff}}$, where τ_{diff} is given by $\tau_{\text{diff}} = V_{\text{th}}^2/D_{\perp\perp}$, $D_{\perp\perp}$ is taken as the value at the origin of velocity space, and v_{th} is the thermal velocity of the Maxwellian component of the unperturbed distribution function.

Fig. 4 shows the distribution function at various stages of evolution. Fig. 4(a) shows the initial distribution. Fig. 4(b) shows the distribution function after it has evolved for one diffusion time. The distribution function resulting from the diffusion simulation shows perpendicular heating of the cold core electrons to energies greater than 500 eV. The heating resulting from our simulation is modest, but does resemble the perpendicularly elongated distribution function displayed in Fig. 1. As we shall discuss in the next section, it is possible that the spectral density is much higher than is indicated in the DE 1 data. Therefore, we include Fig. 4(c), in which we have allowed the simulation to run for three diffusion times. This figure shows that the conic structure is more pronounced, as expected.

5. Conclusions

This work has shown that electron diffusion due to particle interaction with strong AKR can be an effective perpendicular heating mechanism for electrons. The essential physics that enables this process to occur is shown in Figs. 2 and 3. These figures show the effect of warm plasma in lowering the value of the R-X cutoff frequency such that $f_{\text{RX}} < f_{\text{c}}$, as discussed by Winglee (1985) and Wong et al. (1982), enabling the resonant ellipses to encompass the origin of velocity space. The resonant ellipses represent the locus of interaction in velocity space between the electron distribution and the AKR waves. Without the presence of warm plasma, the resonant ellipses would all lie to one side of the $v_\perp$-axis, as shown by Wu (1985), and perpendicular diffusion due to AKR would have little effect on the electron distribution.

The results, shown in Fig. 4, show a good qualitative agreement between the data and the model. In particular, we note a perpendicular stretching of the distribution function combined with some filling of the loss cone. These areas of interaction illustrate the diffusive nature of the interaction: the AKR wave must interact with the perpendicular gradient of the particle distribution. The principal effect of the warm plasma is to place the area of interaction represented by the resonant ellipses in regions of velocity space where there are steep gradients, for example, the origin where the cold plasma core exists and the loss cone.

However, we also note some significant differences between the data and the simulation. The data shown in Fig. 1 indicate that heating occurs most efficiently at intermediate energies, leaving low and high energy components of the distribution nearly unchanged. In our simulation, the high energy distribution was largely unaffected, but the elongation of the low energy distribution was fairly uniform

throughout the low energy part of the distribution. This effect indicates that our diffusion model requires modification, as we now discuss.

Clearly, the approach to heating by diffusion undertaken here is only adequate to give a crude, qualitative result. Some inconsistencies in the present approach are apparent: (1) the assumption of a constant spectral energy density as a function of time; (2) the use of the displaced ring "delta function" distribution function to calculate the index of refraction while using a continuous low energy distribution function as the object of diffusion; and (3) the calculation of the index of refraction at 90° when it is clear that the resonant ellipses can only exist when the angle of incidence is away from the perpendicular. These inconsistencies are computational expedients, suitable only for a preliminary treatment. Clearly, a self-consistent, i.e., a quasilinear approach is needed, but in the present approach we indicate only the plausibility of perpendicular diffusion for the creation of quasiperpendicular conic distributions.

The agreement may be better than appears, however. For example, Figs. 3 and 4 of Menietti et al. (1993) show some heating of the lowest energy electrons. This leads us to think that in the case we present, the heating at low temperatures, which takes place on shorter time scales than that at high temperatures, could be masked by the 6 s integration time of the HAPI instrument and the two-dimensional nature of the observations.

In order to reproduce the saturation time of 0.04 s, we were required to introduce a cold plasma component at an energy no higher than 2.5 eV. However, this value is probably an artificial effect of the resolution of the DE Plasma Wave Instrument. DE PWI has a full spectrum time resolution of 32 s, but as we have seen, the saturation time of AKR is about 0.04 s. The peak spectral density of 10^{-9} $(V/m)^2/Hz$ is an average over many instances of AKR and over a finite bandwidth. In fact, recent observations by the FAST spacecraft have shown very high resolution power spectral densities within the AKR source region as high as 2×10^{-4} $(V/m)^2/Hz$ in short bursts with bandwidths generally less than 1 kHz (Ergun et al., 1998). It is likely that the true peak intensity is much higher than we have indicated. Therefore, it is possible that this mechanism could be effective on distributions at much higher energies.

We have determined the approximate efficiency of the wave heating by calculating the total energy density of the plasma distribution before and after the diffusion. Our results indicate this ratio to be approximately 0.7, 5, and 10% after $t = 1$, 2, and 3 τ_{diff}, respectively. In addition, for 100 eV electrons at a frequency of 60 kHz we estimate heating by AKR to occur up to 100 km away from the source region. This number was determined assuming a power spectral density near the source of 10^{-9} $(V/m)^2/Hz$ which falls off as $1/r^2$. Of course we have already noted that this estimate of the spectral density based on DE-1 time-averaged observations is much less than recently reported short burst observations of the satellite FAST. We thus expect electron heating perpendicular to the magnetic field to be more efficient than we conservatively estimate here. This estimate of heating distance agrees with observations which show "perpendicular conics" approximately 100 km away from the AKR source region.

Perpendicular heating of electrons due to AKR is inherently a warm plasma effect and is expected in regions adjacent to the AKR source region and this is confirmed by observations (cf Menietti et al., 1993; Dory et al., 1998). The generation of quasiperpendicular electron conics near the AKR source, typically at altitudes of 3000 to 5000 km in the nightside auroral region can lead to adiabatic folding of the distribution and perhaps account for a portion of the more typical, smaller pitch-angle, electron conics observed at higher altitudes by DE 1 (cf Menietti et al., 1994, Fig. 8).

Acknowledgements

We would like to thank Dr I. H. Cairns for informative discussions. This research was supported by NASA Grants NAG5-2102 and NAGW-5051.

References

Andre, M., 1993. Electron and ion conics. In: Chang, T., Crew, G.B., Jasperse, J.R. (Eds.), Physics of Space Plasma. Scientific Publishers Inc, Cambridge, MA.

Andre, M., Eliasson, L., 1992. Electron acceleration by low frequency electric field fluctuations: electron conics. Geophys. Res. Lett. 19, 1073.

Bahnsen, A., Jespersen, M., Ungstrup, E., Iversen, I.B., 1987. Auroral hiss and kilometric radiation measured from the Viking satellite. Geophys. Res. Lett. 14, 471.

Bahnsen, A., Pedersen, B.M., Jespersen, M., Ungstrup, E., Eliasson, L., Murphree, J.S., Elphinstone, R.D., Blomberg, L., Holmgren, G., Zanetti, L.J., 1989. Viking observations at the source region of auroral kilometric radiation. J. Geophys. Res. 94, 6643.

Benson, R.F., Calvert, W., 1979. ISIS I observations at the source of auroral kilometric radiation. Geophys. Res. Lett. 6, 479.

Delory, G.T., Ergan, R.E., Carlson, C.W., Muschietti, L., Chaston, C.C., Peria, W., McFadden, J.P., Strangeway, R., 1998. FAST observations of electron distributions within AKR source regions. Geophys. Res. Lett. 25, 2069.

Dory, R.A., Guest, G.E., Harris, E.G., 1965. Unstable electrostatic waves propagating perpendicular to a magnetic field. Phys. Rev. Lett. 14, 131.

Ergun, R.E., Carlson, C.W., McFadden, J.P., Mozer, F.S., Delory, G.T., Peria, W., Chaston, C.C., Temerin, M., Elphic, R., Strangeway, R., Pfaff, R., Cattell, C.A., Klumpar, D., Shelly, E., Peterson, W., Moebius, E., Kistler, L., 1998. Geophys. Res. Lett. 25, 2061.

Eliasson, L., Andre, M., Lundin, R., Pottelette, R., Marklund, G., Holmgren, G., 1996. Observations of electron conics by the Viking satellite. J. Geophys. Res. 101, 13,225.

Gurnett, D.A., 1974. The Earth as a radio source: terrestrial kilometric radiation. J. Geophys. Res. 79, 4227.

Gurnett, D.A., Shawhan, S.D., Shaw, R.R., 1983. Auroral hiss, z mode radiation, and auroral kilometric radiation in the polar magnetosphere: DE 1 observations. Geophys. Res. 88, 329.

Louarn, P., Roux, A., de Feraudy, H., Le Queau, D., 1990. Trapped electrons as a free energy source for the auroral kilometric radiation. J. Geophys. Res. 95, 5983.

Menietti, J.D., 1992. Observations of electron conical distributions and possible production mechanisms. In: Chang, T., Crew, G.B., Jasperse, J.R. (Eds.), Physics of Space Plasmas. Scientific Publishers Inc, Cambridge, MA, p. 465.

Menietti, J.D., Burch, J.L., 1985. Electron conic signatures observed in the nightside auroral zone and over the polar cap. J. Geophys. Res. 90 (A6), 5345–5354.

Menietti, J.D., Weimer, D.R., 1998. DE observations of electric field oscillations associated with an electron conic. J. Geophys. Res. 103, 431.

Menietti, J.D., Burch, J.L., Winglee, R.M., Gurnett, D.A., 1993. DE 1 particle and wave observation in auroral kilometric radiation (AKR) source regions. J. Geophys. Res. 98, 5865.

Menietti, J.D., Weimer, D.R., Andre, M., Eliasson, L., 1994. DE 1 and Viking observations associated with electron conical distributions. J. Geophys. Res. 99, 23,673.

Menietti, J.D., Lin, C.S., Wong, H.K., Bahnsen, A., Gurnett, D.A., 1992. Association of electron conical distributions with upper hybrid waves. J. Geophys. Res. 97 (A2), 1353–1361.

Melrose, D.B., Rönnmark, K.G., Hewitt, R.G., 1982. Terrestrial kilometric radiation: the cyclotron theory. J. Geophys. Res. 87, 5140.

Strangeway, R.J., Kepko, L., Elphic, R.C., Carlson, C.W., Ergun, R.E., McFadden, J.P., Peria, W.J., Delory, G.T., Chaston, C.C., Temerin, M., Cattell, C.A., Möbins, E., Kistler, L.M., Klumpar, D.M., Peterson, W.K., Shelley, E.G., Pfaff, R.F., 1998. FAST observations of VLF waves in the auroral zone: evidence of very low plasma densities. Geophys. Res. Lett. 25, 2065.

Thompson, B.J., Lysak, R.L., 1996. Electron acceleration by inertial Alfven waves. J. Geophys. Res. 101, 5359.

Ungstrup, E., Bahnsen, A., Wong, H.K., Andre, M., Matson, L., 1990. Energy source and generation mechanism for auroral kilometric radiation. J. Geophys. Res. 95 (A5), 5973–5981.

Vlahos, L., Gergely, T.E., Papadopoulos, K., 1982. Electron acceleration and radiation signatures in loop coronal transients. Astrophys. J. 258, 812.

Winglee, R.M., 1985. Effects of a finite plasma temperature on electron cyclotron maser emission. Astrophys. J. 291, 160.

Wong, H.K., Wu, C.S., Ke, F.J., Schneider, R.S., Zieball, L.F., 1982. Electromagnetic cyclotron-loss-cone instability associated with weakly relativistic electrons. J. Plasma Physics 28, 503.

Wu, C.S., 1985. Kinetic cyclotron and synchrotron maser instabilities: radio emission processes by direct amplification of radiation. Space Sci. Rev. 41, 215.

Wu, C.S., Tsai, S.T., Xu, M.J., Shen, J.W., 1981. Saturation and energy-conversion efficiency of auroral kilometric radiation. Astrophys. J. 248, 384.